

A Comparative Study of Different Necking Criteria for Numerical and Experimental Prediction of FLCs

Cunsheng Zhang, Lionel Leotoing, Guoqun Zhao, Dominique Guines, and Eric Ragneau

(Submitted September 30, 2009; in revised form July 9, 2010)

For sheet metal forming, the determination of the onset of localized necking directly influences the formability evaluation and construction of forming limit curves (FLCs). Several necking criteria in the literature have been proposed and widely used, however, there are some restrictions, e.g., some criteria are suitable for numerical methods but not for the experimental phase. In this study, numerical and experimental procedures are carried out to seek an appropriate necking criterion for the prediction of FLCs. This article begins with the FE modeling of the Marciniak test with ABAQUS. Based on the FE simulation, different necking criteria (global and local ones) are reviewed and analyzed in detail, and the FLCs for a 5086 aluminum sheet are constructed with these criteria. On the other hand, a quasi-static experimental Marciniak test is carried out to study the formability for this given sheet. With a chosen necking criterion, the limit strains are experimentally determined. The comparison between experimental and numerical results shows that the chosen necking criterion could be effective to numerically and experimentally evaluate the global formability of this aluminum alloy on the wide range of strain states.

Keywords digital image correlation, forming limit curves, Marciniak test, necking criterion

1. Introduction

Sheet metal forming is a very commonly used method for producing various components of many manufacturing products, especially in automotive or aeronautic industries (Ref 1, 2). However, it is generally bounded by failure limits of the used material corresponding to the onset of localized necking, which limits sheet metal formability. Hence, the determination of the onset of localized necking directly influences the formability evaluation, which is represented by forming limit curves (FLCs) (Ref 3). However, the construction of FLCs is a very complex task, and research on FLCs has always been the subject of extensive experimental, analytical, and numerical studies. Experimental method is a basic and well established way to obtain FLCs of sheet metals. Two main kinds of forming tests have been developed, the so-called out-of-plane stretching [e.g., the Nakazima test (Ref 4), the Hecker test (Ref 5)], and the in-plane stretching [e.g., the Marciniak test (Ref 6)]. For out-of-plane stretching, as illustrated in Fig. 1(a), the blank is deformed under triaxial stress while during in-plane stretching, the stress perpendicular to the sheet surface is small when

compared to the stresses in the plane and could be neglected, hence, the sheet is nearly under plane stress conditions in the central part (see Fig. 1b). However, for experimental determination of FLCs, there is no precise standard to detect the onset of localized necking and construct more stable and reproducible FLCs, in addition to ISO 12004 which is generally considered as too fuzzy (Ref 7).

In recently years, a significant effort has been spent on developing more accurate and reliable analytical and numerical models to construct FLCs (Ref 8-12). Also, several necking criteria have been proposed to predict the onset of localized necking and construct the FLCs of sheet metals, e.g., Brun's criterion (Ref 8), Petek's criterion (Ref 9), Volk's criterion (Ref 10), etc. Although the above failure criteria are widely used, there are some restrictions. If necking occurs, a sharp change of thickness strain can be observed on the plot of thickness strain versus the forming time, Brun's criterion can detect the bifurcation; when a sharp change of thickness strain cannot be clearly observed, this criterion does not function any more (Ref 8), as shown in Fig. 2.

To overcome the limits, the present authors proposed a necking criterion by detecting the intersection point of two bifurcation branches on the plot of thickness strain evolution (Ref 11). With Petek's criterion, one predicts critical moments by calculating the first and second temporal derivatives of the thickness strain (Ref 9). According to Volk's criterion, the onset of localized necking is determined by the two main effects: increase of point number with high strain rate (in the localization area) and decrease of the strain rate outside the localization bands (Ref 10). Later, Situ et al. (Ref 12) determined the onset of localized necking by three different criteria (the commonly used Bragard's criterion (Ref 13), the critical major strain criterion, and the criterion of the maximum second derivative of major strain). They found that the difference in FLCs was largely due to the selection of different failure criteria and pointed out that the criterion of the

Cunsheng Zhang and Guoqun Zhao, Key Laboratory for Liquid-Solid Structural Evolution and Processing of Materials, Ministry of Education, Shandong University, 73 Jingshi Road, Jinan 250061, Shandong Province, People's Republic of China; and Lionel Leotoing, Dominique Guines, and Eric Ragneau, Université Européenne de Bretagne, INSA-LGCGM—EA 3913, 20, Avenue des Buttes de Coësmes, 35043 Rennes Cédex, France. Contact e-mails: zhangcs@sdu.edu.cn and zhaogq@sdu.edu.cn.

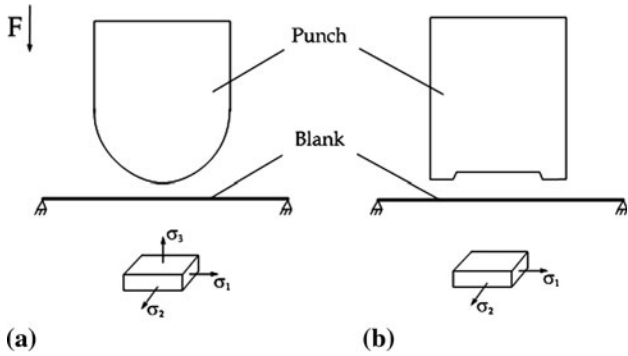


Fig. 1 Comparison of (a) out- and (b) in-plane stretchings

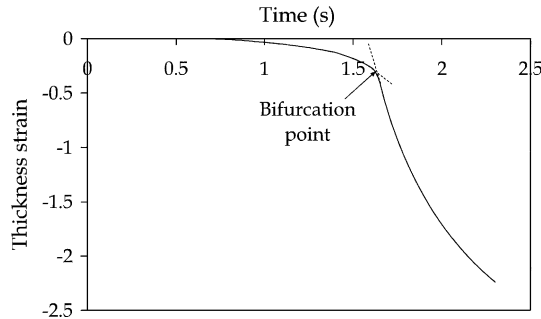


Fig. 2 Plot of thickness strain vs. forming time

maximum second derivative of major strain exhibits more definite physical meaning than other criteria. On the other hand, in the experimental procedure, it is convenient for us to obtain major and minor strains. If one criterion is used to predict the onset of necking based on major and minor strains, it is more suitable for the experimental phase. Therefore, it is seen that some above criteria are suitable for numerical methods but it is too complex to implement for the experimental phase.

Therefore, the principal objective of this study is to compare various necking criteria and choose one which is appropriate for both numerical and experimental prediction of FLCs. First of all, the FE model of the Marciniak test is constructed to numerically study the necking process. With the FE results, different failure criteria (global and local ones) in the literature are reviewed and compared in detail. Then, to experimentally investigate the sheet formability, a reverse experimental apparatus based on the Marciniak test is developed and a quasi-static procedure is carried out for a 5086 aluminum alloy sheet. With the criterion of detection of bifurcation point, the strains corresponding to the onset of localized necking are determined and the FLCs of this sheet are constructed experimentally. Finally, the comparison between the experimental and the numerical results is given and discussed.

2. Construction of FE Model

In this part, the Marciniak test is modeled with ABAQUS. The FE model of the Marciniak test consists of three parts: a rigid cylindrical punch with a flat bottom, a die, and a deformable sheet. In addition, a pressure load is directly applied on the sheet as the blank-holder force (Fig. 3). Keeping the

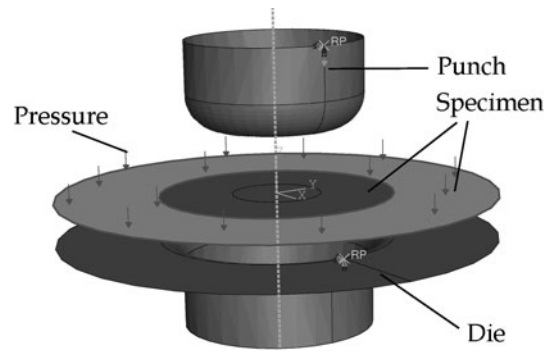
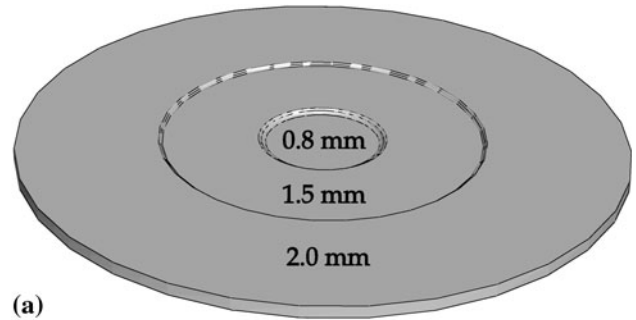
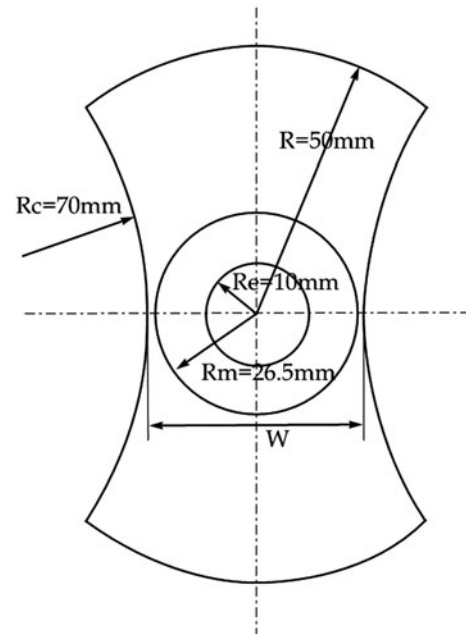


Fig. 3 FE model of the Marciniak test with ABAQUS



(a)



(b)

Fig. 4 (a) Specimen with reduced thickness and (b) specimen geometry

blank in place by means of pressure and friction will be used also in the following experiments (Ref 14).

To trigger localization on the central part of the blank, the specimens are specially designed with a reduced central thickness (0.8 mm) compared to the thickness of the sheet (1.5 mm) and the clamping part (the zone of applied pressure) with a thickness of 2.0 mm, as shown in Fig. 4(a). For the sake of convenience, these three zones are noted as ZT0.8, ZT1.5, and ZT2.0, respectively.

Table 1 Contact interactions of simulation objects in FE analysis

Pieces contacted	Friction coefficient, μ
Punch-ZT0.8	Noncontact
Punch-ZT1.5 and ZT2.0	0.05
Die-blank	0.1

Different specimen geometries are applied to cover different strain states, ranging from uniaxial through plane strain to balanced biaxial tension. All specimens are shaped by cutting strips of different widths W in a circular flange ($R = 50$ mm). The geometry and dimensions of specimen used here are shown in Fig. 4(b). R_e and R_c are the radius of the 0.8 and 1.5 mm zones, respectively. In this article, the values of W are taken from 10 to 100 mm.

Due to symmetrical boundary conditions, only one quarter of the model is simulated. The analysis is carried out with shell linear elements S4R. The contact interactions between the surfaces of the FE model are defined with Coulomb's friction law. The friction coefficients (μ) among the simulation objects in contact have the values in Table 1. There is no friction between the punch and the central part of specimen, which is under the identical condition to the following experimental procedure.

For numerical simulation, aluminum alloy 5086 is chosen and the material behavior of the AA5086 sheet has been characterized by tensile tests. To define the elastic properties of material, Young's modulus is taken as 66120 MPa and Poisson's ratio is taken as 0.389. The experimental true stress-true strain curve, obtained from a tensile uniaxial test, is implemented in the FE code for simulation.

3. Comparison of Different Necking Criteria

Here, we take the specimen of width 40 mm as an example to analyze this simulation process and to determine the onset of localized necking. To study the history of deformation and localization, two typical elements: Element B in the localized site and Element A in the vicinity are chosen as illustrated in Fig. 5. Due to the reduced thickness of the central part, localized necking generally occurs at the center of the sheet. In the following part, different necking criteria in the literature will be reviewed and compared in detail.

3.1 Equivalent Plastic Strain Increment Ratio (CRIT1)

Figure 6 presents the evolutions of the equivalent plastic strain of Elements A and B. It is noteworthy that homogeneous deformation takes place for the two elements until a divergence occurs at approximately $t = 1.6$ s (t is the forming time). After a certain moment, the equivalent plastic strain in the localized zone rises extremely rapidly while the non-localized zone (Element A) shows saturation in the equivalent plastic strains. The necking ultimately ends with the formation of a rupture at a very small area in the localized zone (Element B).

The equivalent plastic strain increment ratio of two elements is calculated and plotted in Fig. 7. The plastic strain increment ratio for elements inside and outside the localized site demonstrates two distinct relationships before and after the

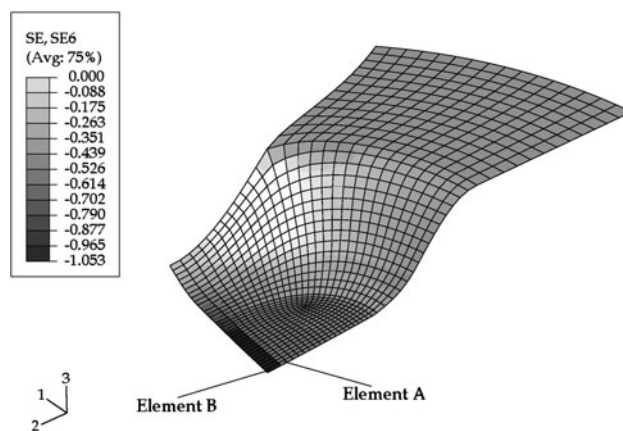


Fig. 5 Distribution of thickness strain in the specimen

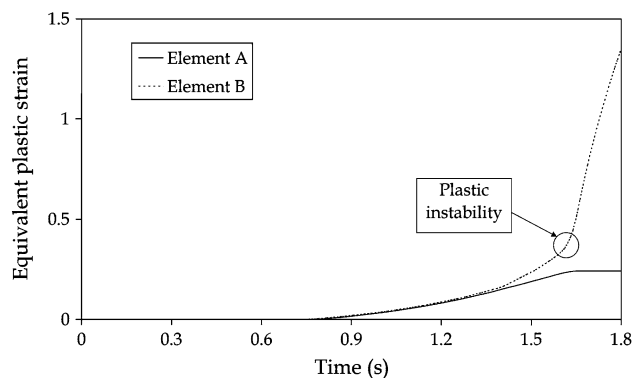


Fig. 6 Evolutions of the equivalent plastic strain in Elements A and B

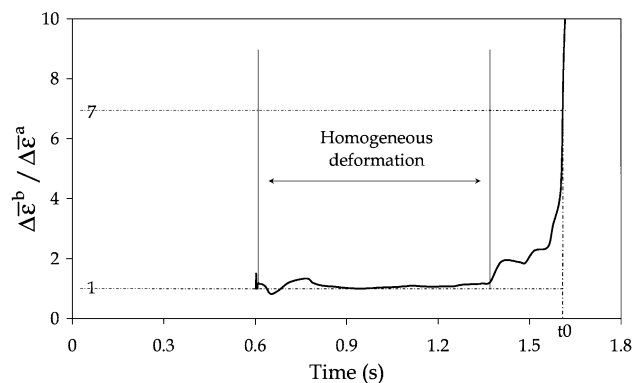


Fig. 7 Evolution of equivalent plastic strain increment ratio of Element B versus Element A

onset of localized necking. The ratio increases rapidly after a certain moment. Here, localized necking is assumed to occur when this value attains 7 [a usual value adopted in the M-K model (Ref 15)]. The major and minor strains of Element B corresponding to this moment are calculated by linear interpolation of closely calculated strain values and could be noted as a point $(-0.056, 0.32)$ on the FLC. By changing the specimen geometry, limit strains of all specimens are determined with CRIT1 as displayed in Fig. 12.

3.2 Maximum Second Temporal Derivative of Thickness Strain (CRIT2)

If localized necking occurs, the thickness strain in localized site suffers a drastic change, i.e., it undergoes a great velocity of deformation. Therefore, the deformation evolution of a localized element can be described by the first and the second time derivatives, i.e., the strain rate and the strain acceleration, respectively (Ref 9, 12). The maximum of the strain acceleration is assumed to correspond to the onset of localized necking, and the reduction in the strain acceleration from maximum to zero represents the process of localization. In the mean time, the strain rate increases to maximum and the strain keeps increasing until fracture occurs.

Here, the strain rate and the strain acceleration (represented by $\dot{\epsilon}_{33}$ and $\ddot{\epsilon}_{33}$) in Element B are calculated and plotted in Fig. 8. The figure shows that the moment corresponding to the peak of strain rate ($t_1 = 1.66$ s) is later than that of strain acceleration ($t_2 = 1.64$ s). According to Petek et al. (Ref 9) and Situ et al. (Ref 12), the limit strains $(-0.064, 0.42)$ corresponding to the peak (t_2) are retained as a point on the FLC. The limit strains for all specimens determined with CRIT2 are shown in Fig. 12.

3.3 Transition of Strain Path (CRIT3)

As mentioned previously, at the beginning of localized necking, a sharp change of thickness strain ϵ_{33} can be observed in the localized zone, while the minor strain remains almost constant ($\Delta\epsilon_{22} = 0$). Therefore, the transition of the deformation condition to a relative plane strain condition ($\Delta\epsilon_{22}/\Delta\epsilon_{11} = 0$) can be used as a local criterion to determine the onset of localized necking.

In Fig. 9, the evolutions of $\Delta\epsilon_{22}/\Delta\epsilon_{11}$ of Elements A and B are plotted. It can be seen that the evolutions in the two elements are relatively similar till $t = 1.65$ s. After this moment, $\Delta\epsilon_{22}/\Delta\epsilon_{11}$ in Element A changes rapidly, while in

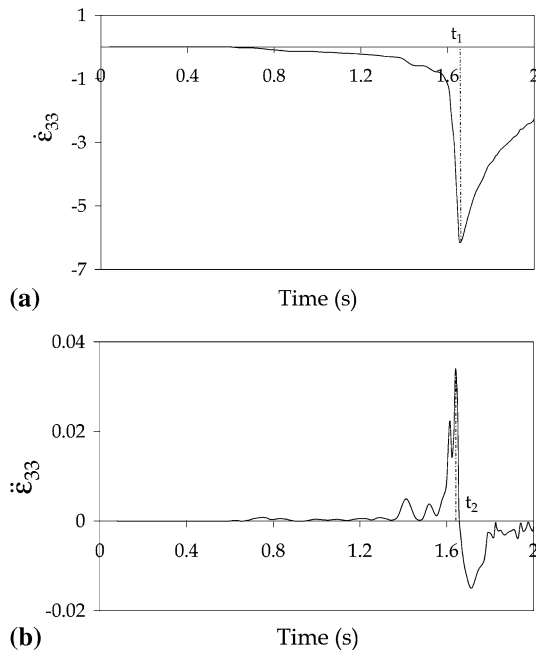


Fig. 8 (a) First derivative of the thickness strain and (b) second derivative of thickness strain

contrast, that in Element B tends to zero. With this criterion, plastic instability occurs at $t = 1.65$ s, and the corresponding limit strains for this specimen are $(-0.066, 0.51)$. Please found the limit strains determined with CRIT3 in Fig. 12.

3.4 Maximum Punch Force (CRIT4)

During a tensile test, the point of plastic instability generally appears as the force begins to drop after the maximum force has been reached. Therefore, the peak force can sometimes be used as a global criterion to predict the onset of localized necking. On the plot of punch force versus time during the simulation, a peak moment is assumed to occur at the onset of localized necking. With this global criterion, CRIT4, the limit strains for all specimens are shown in Fig. 10.

As seen from the numerical results, this global criterion sometimes gives much overestimated prediction of sheet formability and no forming limit curves can be observed. This observation agrees with Petek's conclusion that the forming force is a general parameter and is therefore probably not the most suitable one to describe the local deformation behavior of sheet metal (Ref 9).

3.5 Detection of Bifurcation Point (CRIT5)

As the occurrence of plastic instabilities is determined by localized necking with size of the order of the sheet thickness, the thickness strain can be used as a local criterion to evaluate the occurrence of necking. If necking occurs, a sharp change of thickness strain can be observed. From this moment on, the

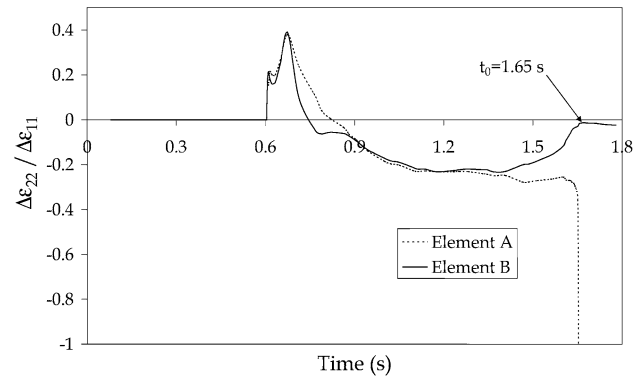


Fig. 9 Evolution of strain paths of Elements A and B

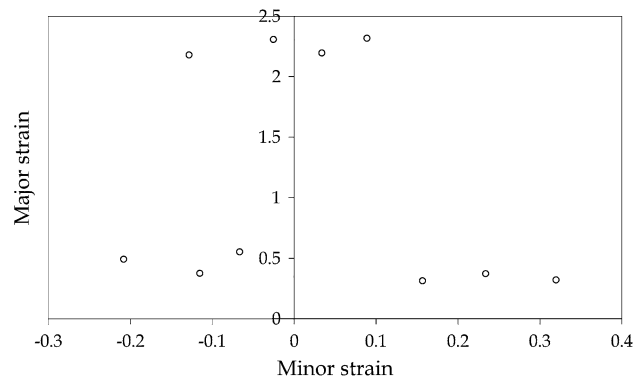


Fig. 10 Limit strains of AA5086 sheet determined by CRIT4

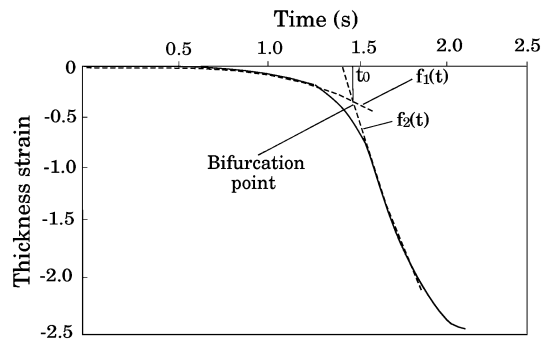


Fig. 11 Detection of bifurcation point by fitting

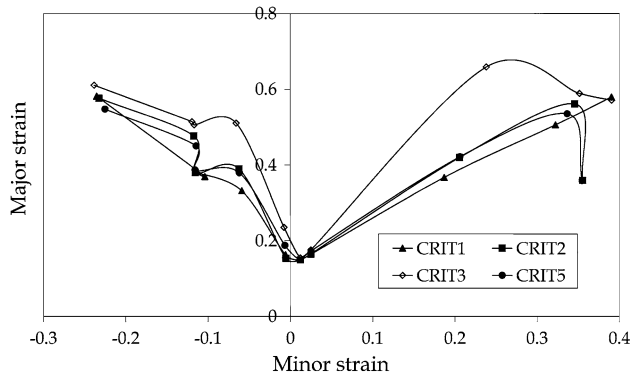


Fig. 12 FLCs of AA5086 determined with different failure criteria

evolution of thickness strain will be drastic (Fig. 2). The onset of plastic instability corresponds to a bifurcation point, i.e., the intersection point of two bifurcation branches (Ref 11). When a sharp change of thickness strain cannot be clearly observed, as shown in Fig. 11, a polynomial curve fitting method is proposed. Here, $f_1(t)$ and $f_2(t)$ are two third degree polynomial functions which provide fitting curves of the two branches. Through calculation and analysis, the two functions can be described as follows:

$$f_1(t) = -0.113t^3 + 0.108t^2 - 0.027t + 0.0013 \quad (\text{Eq 1})$$

$$f_2(t) = -2.59t^3 + 18.51t^2 - 45.27t + 35.51 \quad (\text{Eq 2})$$

The time coordinate of the intersection point is calculated as $t = 1.62$ s. The major and minor strains corresponding to the moment t are obtained by linear interpolation ($-0.062, 0.37$). Following this procedure, all limit strains could be obtained with CRIT5, as shown in Fig. 12.

3.6 Comparison of Numerical FLCs with Different Failure Criteria

For this given specimen, limit strains and corresponding moments determined with different failure criteria are summarized in Table 2.

As seen from the table, different failure criteria give different predictions of limit strains, especially for global and local ones. Although there are no significant discrepancies between the critical moments determined by different criteria, the points on the FLCs may be quite different as shown in

Table 2 Limit strains and corresponding moments with different failure criteria

	CRIT1	CRIT2	CRIT3	CRIT4	CRIT5
t, s	1.60	1.64	1.65	1.66	1.62
ε_{11}	0.32	0.42	0.51	0.55	0.37
ε_{22}	-0.056	-0.064	-0.066	-0.067	-0.062

Fig. 12. Hence, to properly determine formability of sheet metals, it is essential and crucial to choose an appropriate criterion.

From the above comparison, several conclusions can be drawn:

- (1) The only global criterion (CRIT4) leads to very different prediction of FLC (Fig. 10) compared with the local ones. Indeed, the sheet formability is greatly overestimated, and no forming limit curve clearly appears. Hence, forming force is probably not suitable to describe the deformation behavior of sheet metals, and for determining the onset of localized necking, local failure criteria are more precise than the global one.
- (2) The local criterion CRIT3 shows a slightly higher prediction than the three others. The reason for the difference might result from the difficulty of determining the moment of transition of deformation to plane strain condition. In addition, this criterion is not valid at or near plane strain condition.
- (3) There is a good agreement between the FLCs determined by the criteria CRIT1, CRIT2, and CRIT5. Differently from CRIT2, CRIT1, and CRIT5 predict the onset of localized necking with the principal strains, hence, they are easy to use for experimental determination of FLCs.

4. Experimental Validation and Discussions

To experimentally investigate sheet formability and validate the above numerical results, a reverse experimental apparatus based on the Marciniak test is developed in this study, as shown in Fig. 13. During the experiments, the die with the clamped specimen moves downwards and the fixed punch stretches the sheet. With this reverse experimental setup, in which the specimen is formed over the punch until fracture appears in the surface of the specimen, the distance between the mirror and the specimen is constant throughout the test. This allows the camera to be focused on the specimen surface and take sequential pictures.

Figure 14 shows the complete experimental apparatus, which includes a 3369 INSTRON tensile testing machine (50 kN load capacity and crosshead speed range of from 0.005 to 500 mm/min), the Marciniak test setup and an image acquisition system. A compressive force is applied to the sheet samples during the experiments, and the test control system records the force and the displacement of the crosshead. To obtain sufficient and reliable data, more specimen geometries in experiments are used than during the numerical procedure, as displayed in Fig. 15.

The DIC technique associated with a high-speed camera is used to evaluate the strains on the specimen surface. To perform correlation analysis for obtaining the surface strains in this study, the commercial digital imaging program CORRELA2006 is employed, which is developed by LMS at the University of Poitiers. Here, based on the above analysis in Sect. 3, due to its simplicity, CRIT1 (equivalent plastic strain increment ratio) is chosen as a criterion to determine the onset of localized necking. By testing different specimens according to Fig. 15, limit strains of the AA5086 sheet could be determined by experiments as shown in Fig. 16.

Figure 17 displays limit strains determined by numerical and experimental methods. The comparison shows that there is much discrepancy between experimental and numerical limit

stains, especially at the left-hand side on the FLCs, the strain states with the experimental procedure are located in a narrower range. This phenomenon maybe result from the absent of lubricants during the experiments, which influences the strain path. The agreement between the experimental and the numerical results is not perfect but the both methods permit to well model the global formability of this aluminum alloy on the wide range of strain states. In fact, the scatter of experimental data is inevitable, in view of the data scatter present when characterizing the formability of a material with experimental procedure, some researchers, such as Janssens et al. (Ref 16), have proposed forming limit bands (FLB) instead of FLC. Considering lubricant effects, not presented in this study, should improve the determination of sheet formability and improve the agreement between both the methods. Hence, it is concluded that the chosen criterion can be used for the numerical and experimental prediction of FLCs. Also, the experimental setup developed in this article works well to experimentally investigate the sheet formability.

5. Conclusion

This study combined the numerical and the experimental procedures to seek an appropriate necking criterion for the

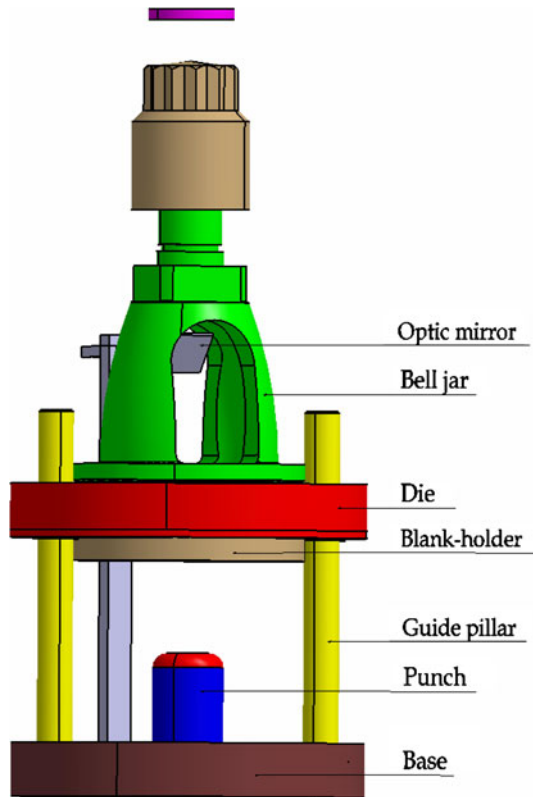


Fig. 13 Model of the Marciniak test setup

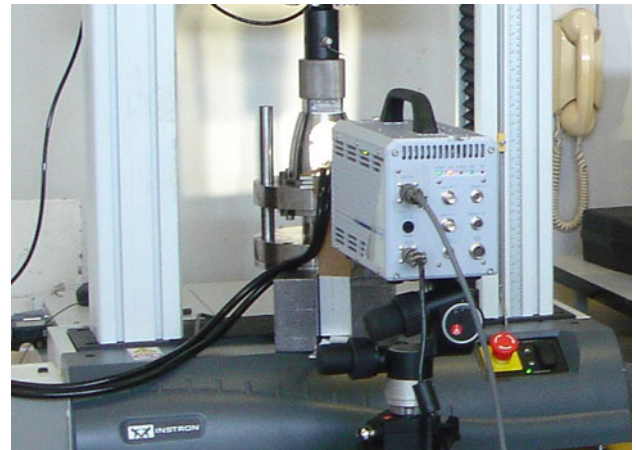


Fig. 14 Experimental apparatus of the Marciniak test

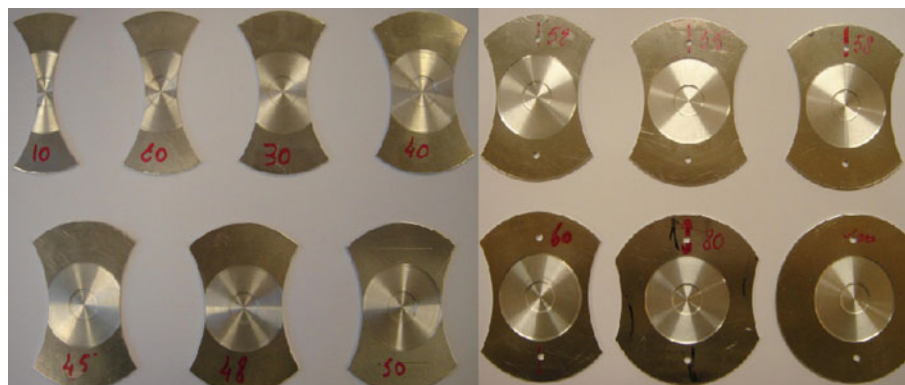


Fig. 15 Specimens used in the experiments

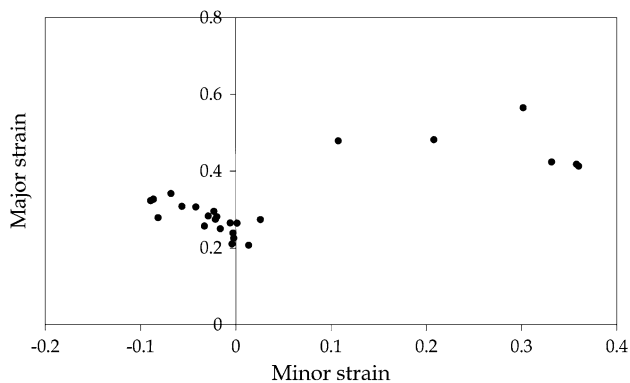


Fig. 16 Experimental FLC of AA5086 sheet with CRIT1

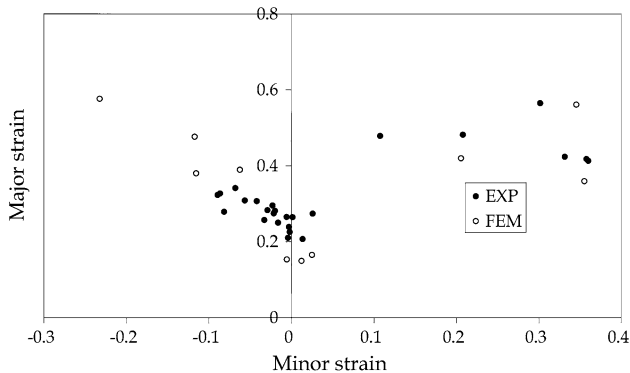


Fig. 17 Comparison of limit strains determined by numerical and experimental methods

prediction of FLCs of sheet metals. By FE modeling of the Marciniak test and carrying out the experimental Marciniak test, the conclusions are drawn as follows:

- (1) With the numerical simulation of the modified Marciniak test, different failure criteria (global and local ones) of localized necking in the literature are reviewed and compared in detail. The comparison shows that forming force is probably not suitable to describe the deformation behavior of sheet metals, and for determining the onset of localized necking, local failure criteria are more precise than the global one. Moreover, due to the difficulty in determining the moment of transition of deformation to plane strain condition, the local criterion CRIT3 (transition of strain path) shows a slightly better prediction than the other local criteria. Furthermore, the criterion of equivalent plastic strain increment ratio (CRIT1) and criterion of detection of bifurcation point (CRIT5) are easy to use for experimental determination of FLCs.

- (2) A modified Marciniak test has been developed in this study to experimentally investigate the sheet formability and validate the numerical results. With the chosen necking criterion, the limit strains are obtained. Though the agreement between the experimental and the numerical results is not perfect, both methods permit to effectively evaluate the global formability of this aluminum alloy on the wide range of strain states. It is concluded that the chosen criterion can be used for the numerical and the experimental prediction of FLCs.

References

1. C.L. Chow, M. Jie, and S.J. Hu, Forming Limit Analysis of Sheet Metals Based on a Generalized Deformation Theory, *J. Eng. Mater. Technol.*, 2003, **125**, p 260–265
2. W.F. Hosford and J.L. Duncan, Sheet Metal Forming: A Review, *J. Miner. Met. Mater. Soc.*, 1999, **51**(11), p 39–44
3. S.P. Keeler and W.A. Backofen, Plastic Instability and Fracture in Sheets Stretched Over Rigid Punches, *Trans. ASM*, 1963, **56**, p 25–48
4. K. Nakazima, T. Kikuma, and K. Asuka, Study on the Formability of Steel Sheets. Technical Report, Yawata, 1971
5. A.K. Ghosh and S.S. Hecker, Stretching Limits in Sheet Metals: In-Plane Versus Out-Of-Plane Deformation, *Metall. Trans.*, 1974, **5**, p 2161–2164
6. Z. Marciniak, K. Kuczynski, and T. Pokora, Influence of the Plastic Properties of the Material on the Forming Limit Diagram for Sheet Metal Tension, *Int. J. Mech. Sci.*, 1973, **15**, p 789–805
7. A. Col, Numerical and Experimental Methods of Forming Limit Curves Prediction for the Processes of Stamping and Hydroforming of Tubes, *Proceedings of the FLC-Zurich 06*, Zurich, Switzerland, 2006
8. R. Brun, A. Chambard, M. Lai, and P. De Luca, Actual and Virtual Testing Techniques for a Numerical Definition of Materials, *Proceedings of NUMISHEET '99*, Besancon, France, 1999, p 393–398
9. A. Petek, T. Pepelnjak, and K. Kuzman, An Improved Method for Determining Forming Limit Diagram in the Digital Environment, *J. Mech. Eng.*, 2005, **51**, p 330–345
10. W. Volk, New Experimental and Numerical Approach in the Evaluation of the FLD with the FE-Method, *Proceedings of the FLC-Zurich 06*, Zurich, Switzerland, 2006
11. C.S. Zhang, L. Leotoing, D. Guines, and E. Ragneau, Theoretical and Numerical Study of Strain Rate Influence on AA5083 Formability, *J. Mater. Process. Technol.*, 2009, **209**, p 3849–3858
12. Q. Situ, M. Jain, and M. Bruhis, A Suitable Criterion for Precise Determination of Incipient Necking in Sheet Materials, *Mater. Sci. Forum*, 2006, **519–521**, p 111–116
13. R. Arrieux, “Détermination Théorique et Expérimentale des Courbes Limites de Formage en Contraintes”, PhD thesis, INSA de Lyon, 1990
14. C.S. Zhang, “Investigations on the Effect of Strain Rate Sensitivity on Formability of Aluminium Alloy Sheets,” PhD thesis, INSA de Rennes, France, 2008
15. D. Banabic, S. Comsa, P. Jurco, G. Cosovici, L. Paraianu, and D. Julean, FLD Theoretical Model Using a New Anisotropic Yield Criterion, *J. Mater. Process. Technol.*, 2004, **157–158**, p 23–27
16. K. Janssens, F. Lambert, S. Vanrostenberghe, and M. Vermeulen, Statistical Evaluation of the Uncertainty of Experimentally Characterised Forming Limits of Sheet Steel, *J. Mater. Process. Technol.*, 2001, **112**, p 174–184